

Cosmology, AGN and MATISSE

Romain G. Petrov, James Leftley,

Niklas Moszczynski, Pierre Vermot

Lagrange Laboratory, University Côte d'Azur, OCA, CNRS

With the HFT team: Fatmé Allouche, Stéphane Lagarde, Abdelkarim Boskri,
Massinissa Hadjara, Amokrane Berdja

With some inspiration from the MATISSE and GRAVITY+ AGN groups

H0 tension

Use the Λ CDM standard cosmological model:

$$H_0 = 67.49 \pm 0.5$$

Direct distance measurements:

$$H_0 = 73.17 \pm 0.86$$

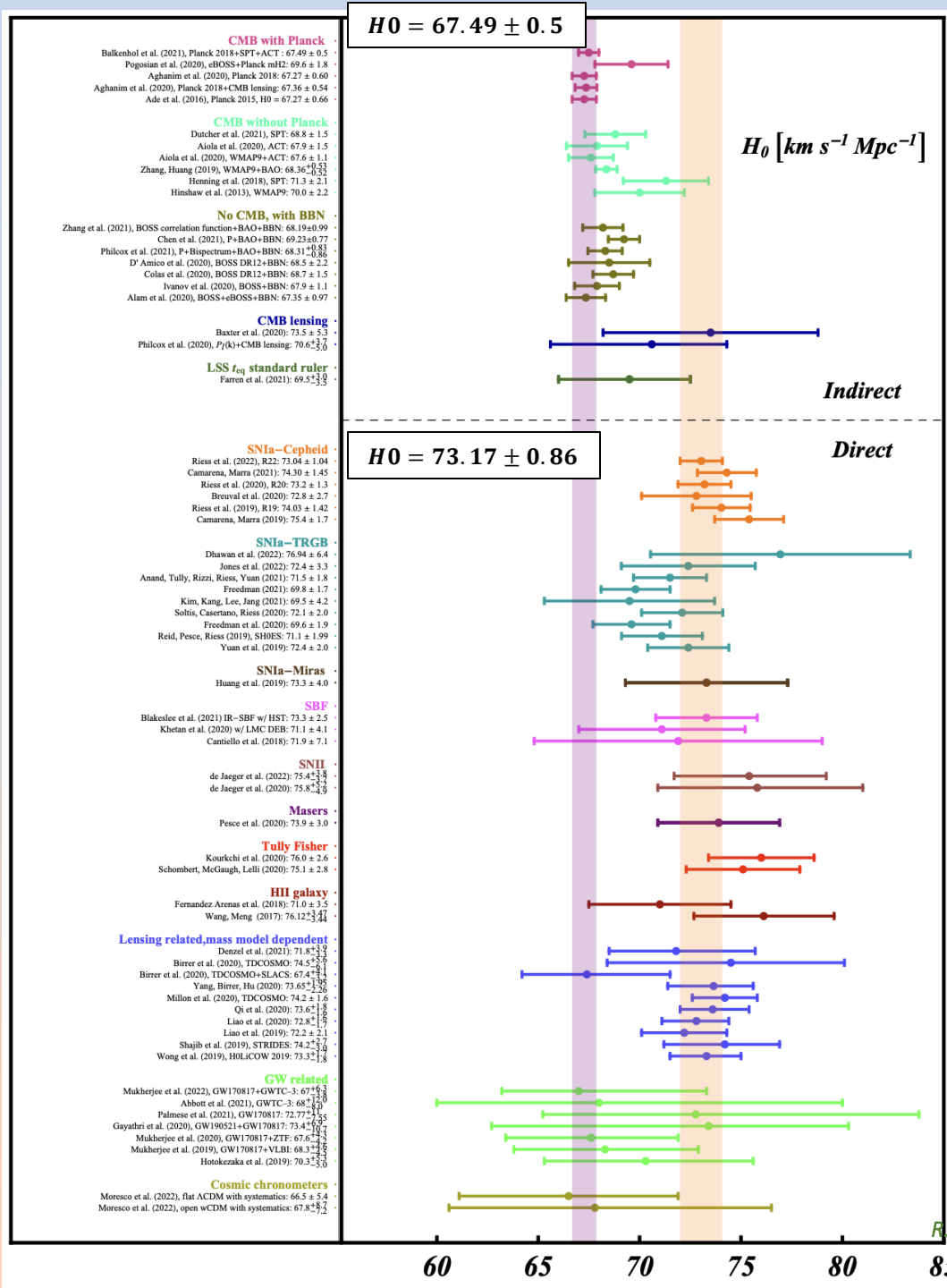
(update Breuval+, ApJ 2024)

Riess+, ApJ 1999: H0 Tension \leftrightarrow New Physics
« Possible physics causes for a 2%–4% change in H0 include time-dependent dark energy or nonzero curvature, while a larger 5%–8% difference may come from dark matter interaction, early dark energy or additional relativistic particles. »

Very high interest of a:

- Geometrical distance measurement
- With 1% accuracy at low redshift ($z < 0.2-0.4$)
- With 10% accuracy up to $z \sim 1.5$

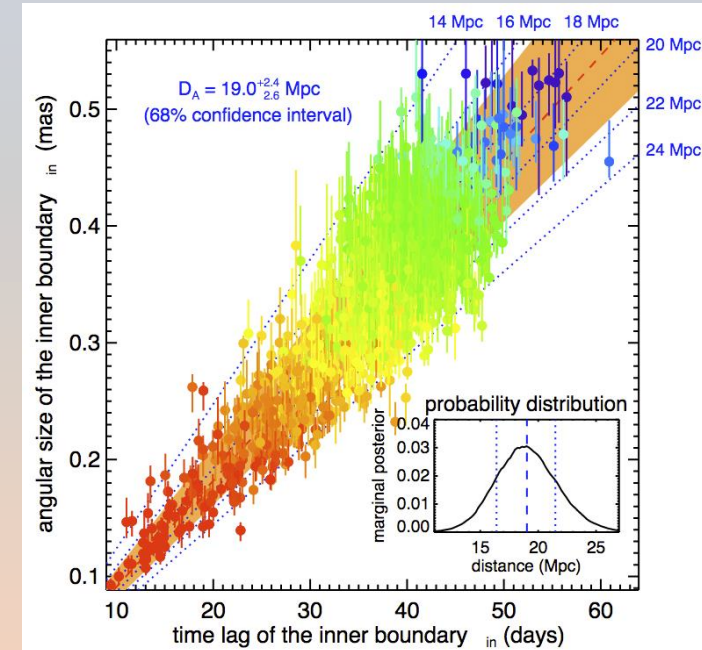
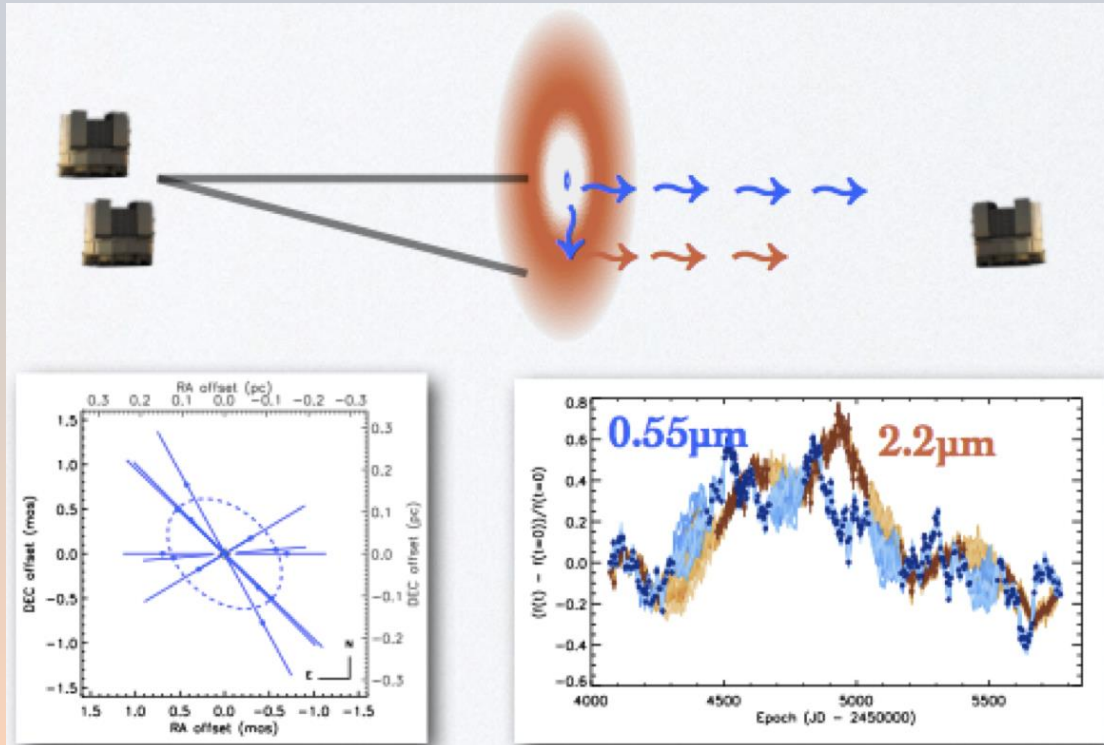
From « Cosmology intertwined: A review of the particle physics, astrophysics, and cosmology associated with the cosmological tensions and anomalies », Abdalla, E. and 202 co-authors, JHEAp, 34, 2022



$z < 0.15$ 1% accuracy
Multi objects statistics
Absolute luminosity + a few geometrical anchors

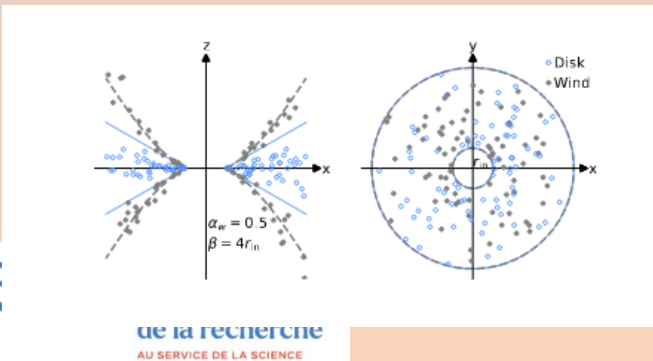
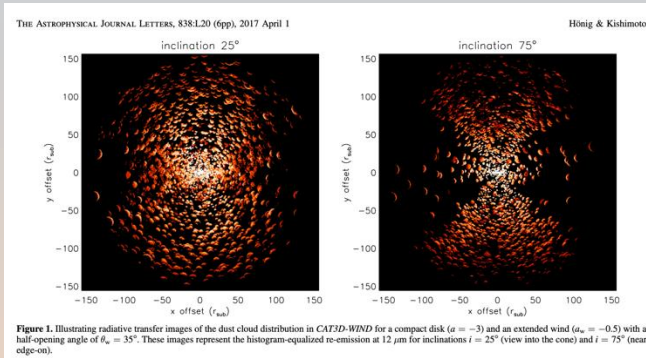
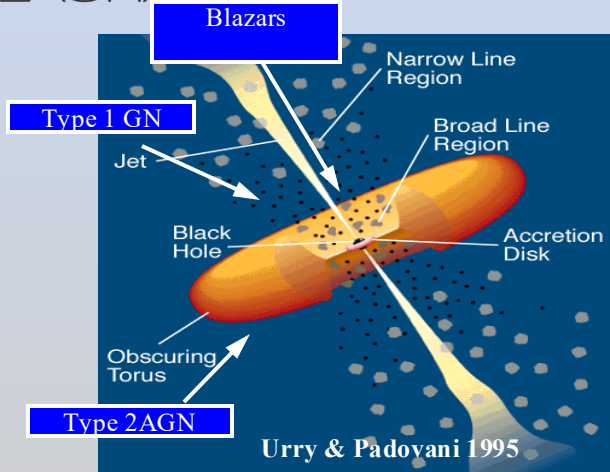
$z \sim 1-1.5$ 5-10% accuracy
Lensing and GW
Individual objects

- Karovska & Elvis (2003): linear size from Reverberation Mapping + Angular Size from interferometry → parallax
 - Dreams of 500 m baselines in the visible to resolve BLRs
- Petrov et al (2000 & 2012): (only) differential interferometry can resolve BLRs on the VLT
- Hönig (2014): dust parallax: NGC 4151 at 19 ± 2.5 Mpc (13%)
 - Very suitable for MATISSE but for the number of targets (and the dust complexity)



Hönig+, Nature, 2015

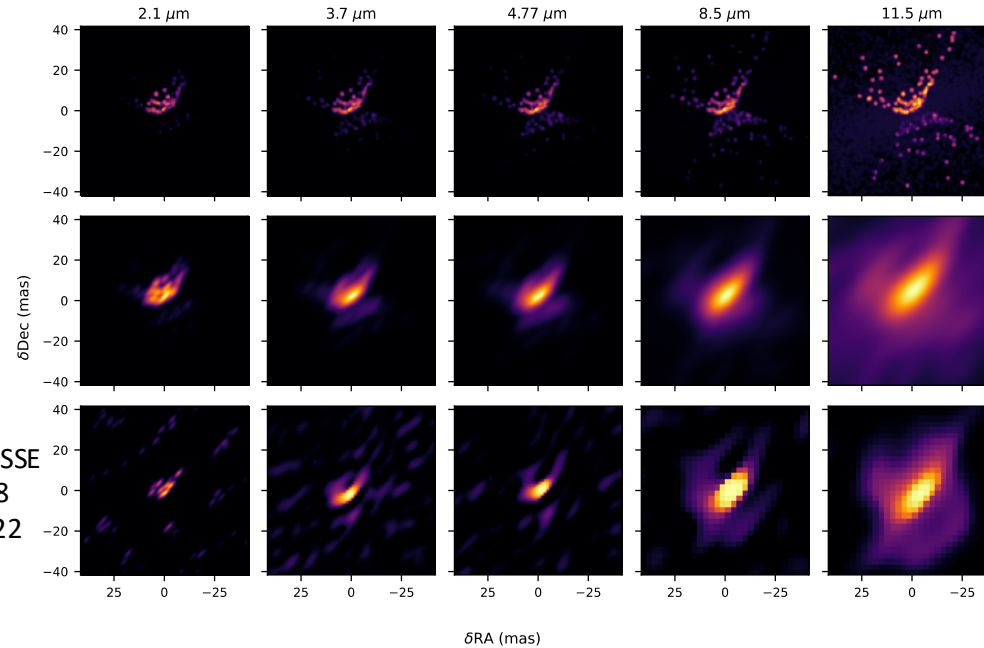
Active Galactic Nuclei



Toward an update of the unified model from panchromatic observations and models ?

Torus + dusty wind panchromatic model (Leftley+, 2023)

GRAVITY and MATISSE images of NGC1068 Gamez-Rosas+, 2022 Gravity Coll+, 2019



Circinus Galaxy

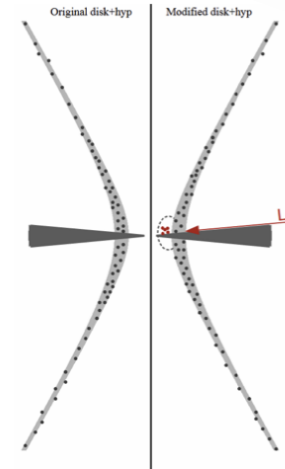
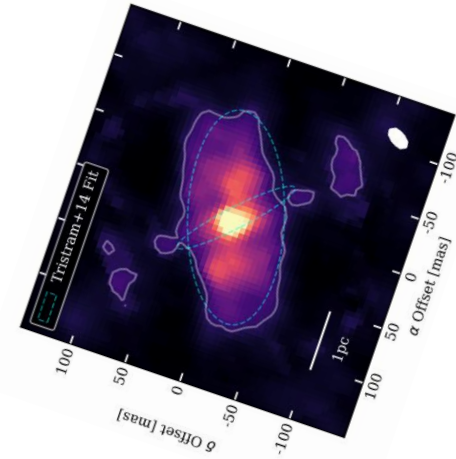


Fig. 6. Schematic of the dust within the RT models that best reproduce the observed dust temperatures. The basis of the model comes from Sialevski et al. (2019), and a rough parameter range is given in Paper I. Here we have added a cluster of dust clouds above the disk and behind the hyperbolic cone, at a position that in projection corresponds to the central aperture. These clouds could represent, for example, a puffed-up sublimation zone, freshly launched winds, or a smoother boundary for the hyperbolic cone. The spatial resolution of these observations is not sufficient to distinguish between these scenarios.

Isbell+, 2024

For an non-resolved source:

The phase (or the photocenter) gives the relative position (in the direction of the baseline) of each velocity (or wavelength) bin through an emission line.

The visibility gives the relative sizes projected on the baseline) of each bin.

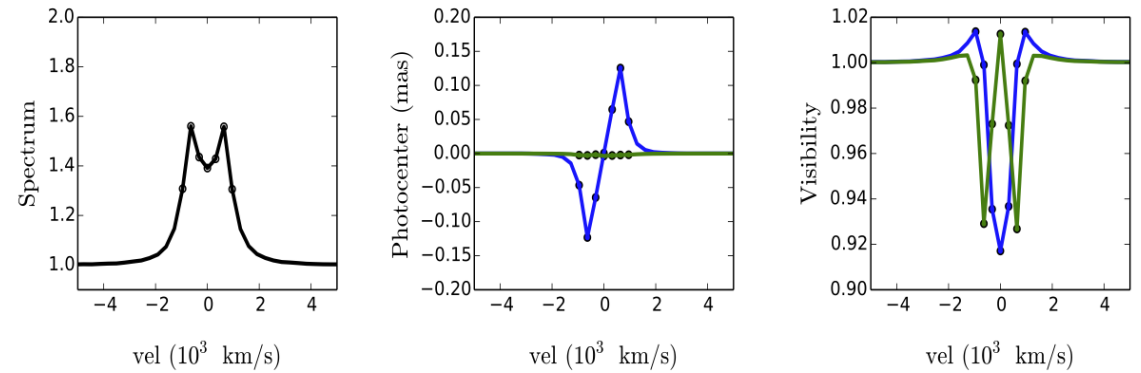
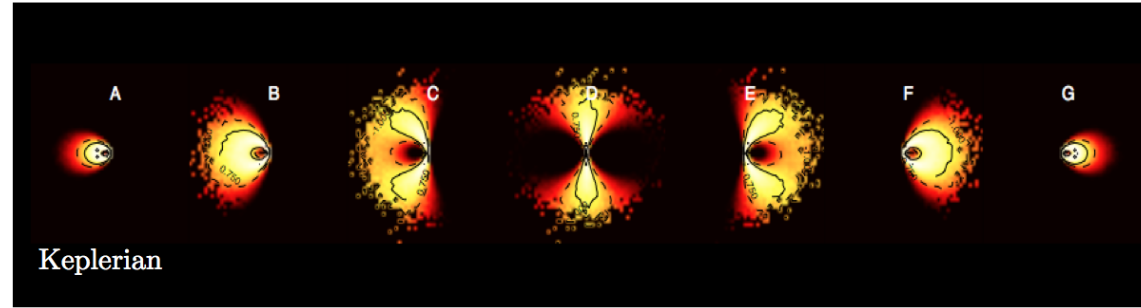


FIGURE 4.4: Line intensity map (upper panel) across the emission line for a flat Keplerian velocity field for seven different spectral channels (top panel). Emission line profile is shown in lower-left panel. Photocenter displacement (lower-middle) and visibility (lower-right) in parallel to the rotation axis (green) and perpendicular to the rotation axis (blue) with spectral resolution $R = 1500$. This model is computed considering a thin Keplerian disk $\sigma_{\text{blr}} = 0.4$ and $i = 30^\circ$.

Rakshit, MNRAS 2015 and Thesis

For an non-resolved source:

The phase (or the photocenter) gives the relative position (in the direction of the baseline) of each velocity (or wavelength) bin through an emission line.

The visibility gives the relative sizes projected on the baseline) of each bin.

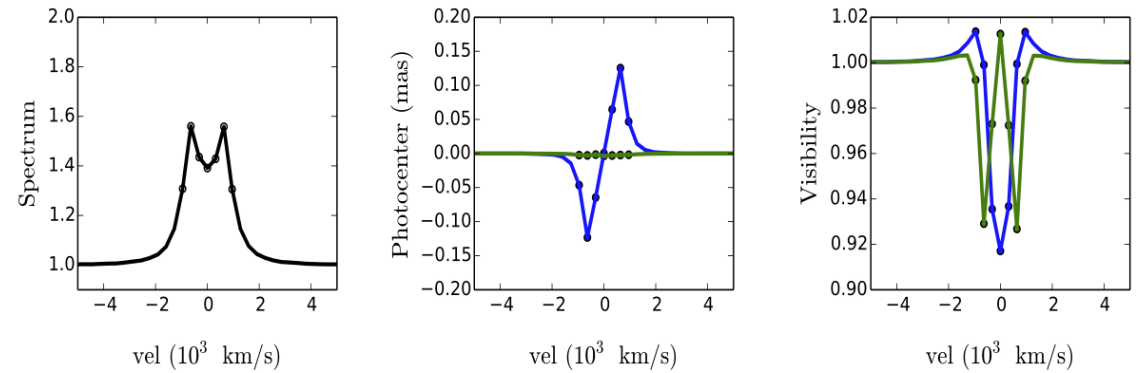
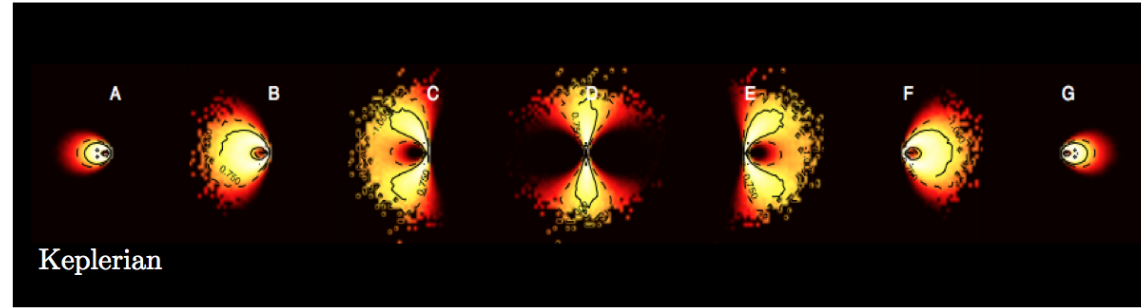
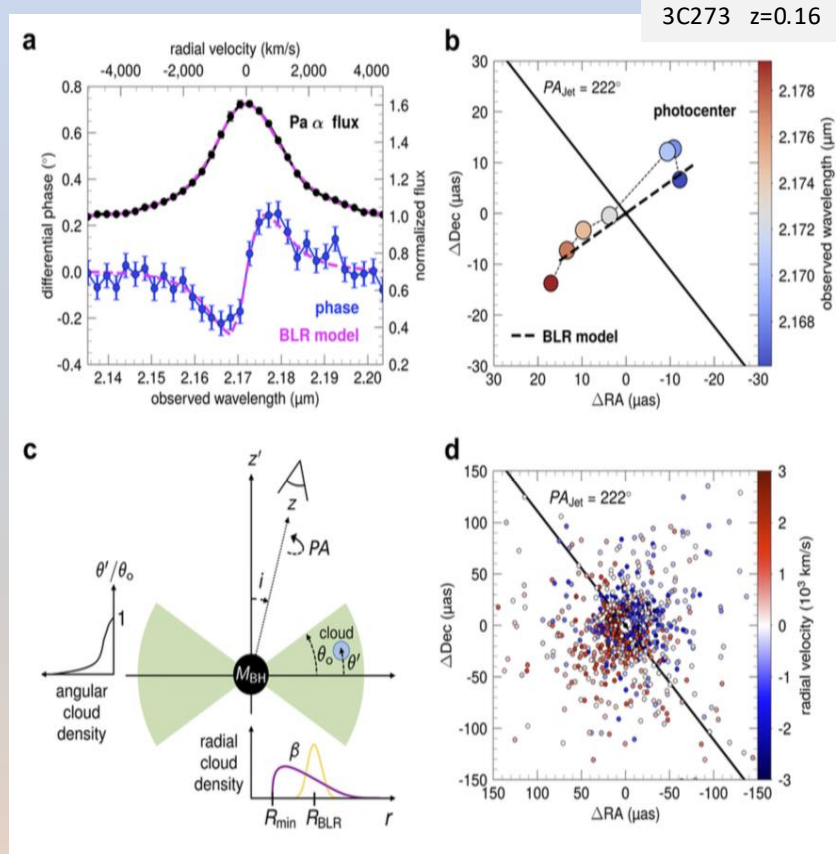


FIGURE 4.4: Line intensity map (upper panel) across the emission line for a flat Keplerian velocity field for seven different spectral channels (top panel). Emission line profile is shown in lower-left panel. Photocenter displacement (lower-middle) and visibility (lower-right) in parallel to the rotation axis (green) and perpendicular to the rotation axis (blue) with spectral resolution $R = 1500$. This model is computed considering a thin Keplerian disk $\sigma_{\text{blr}} = 0.4$ and $i = 30^\circ$.

Rakshit, MNRAS 2015 and Thesis

- BLR parallax method
 - Spectro-Astrometry on the VLTI → angular BLR size
 - Line Reverberation Mapping → linear BLR size
 - A few targets with ~15% accuracy
- GRAVITY+ → Spectro-astrometry on hundreds of targets up to $z > 3$
- 100 targets with 15% accuracy → 1.5%
 - If we can remove the geometric biases
 - If all targets have <15% accuracy
 - If we can combine Spectro Astrometry and Reverberation Mapping on the same targets



GRAVITY collaboration+, Nature, 2018

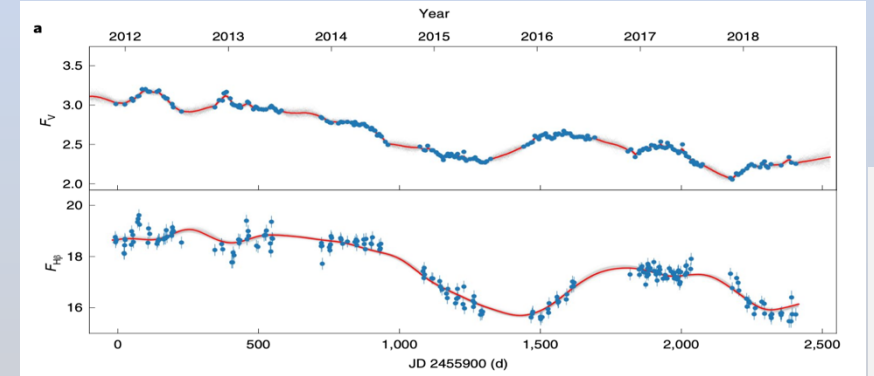
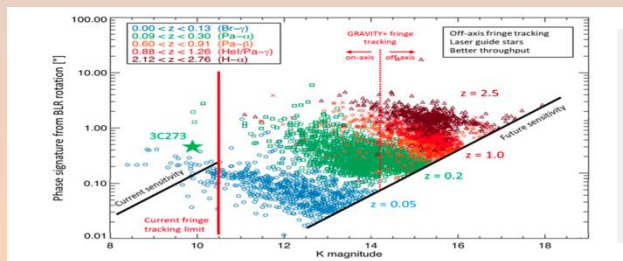


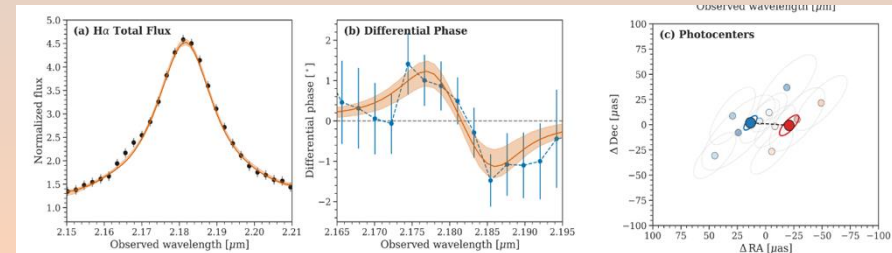
Table 1 | Parameters used in the BLR model and the SARM results of 3C 273

Parameters	Meanings	GRAVITY	RM ¹⁰	Joint analysis	Prior ranges
F	Fractional inner radius of the BLR	$\sqrt{(0.23 \pm 0.08)}$	✓	$0.49^{+0.12}_{-0.20}$	[0, 1]
β	Radial distribution shape parameter	$\sqrt{(1.4 \pm 0.2)}$	✓	$1.09^{+0.91}_{-0.40}$	[0, 4]
$\theta_{\text{out}} (^{\circ})$	Half opening angle of the BLR	$\sqrt{(45^{+9})}$	✓	$39.96^{+4.01}_{-3.72}$	[0, 90]
$i_0 (^{\circ})$	Inclination angle of the BLR	$\sqrt{(12 \pm 2)}$	✓	$8.41^{+0.99}_{-0.91}$	[0, 90]
$PA (^{\circ})$	Position angles	$\sqrt{(210^{+6}_{-9})}$		$210.99^{+3.67}_{-4.63}$	[0, 360]
R_{BLR} (light day)	Averaged linear sizes		✓	$184.17^{+6.77}_{-8.57}$	[1, 10 ³]
M_* (10 ⁸ M _⊙)	Supermassive black hole mass	2.6 ± 1.1		$5.78^{+1.11}_{-0.88}$	[10 ⁻² , 10]
D_* (Mpc)	Absolute angular distance	550 (assumed)		$551.50^{+92.31}_{-78.3}$	[10, 10 ⁴]
ξ_{BLR} (μas)	Averaged angular sizes	$\sqrt{(46 \pm 10)}$		$59.70^{+39.9}_{-10.31}$	
ζ (10 ⁻³)	Dimensionless velocity parameter	$\sqrt{(1.01 \pm 0.22)}$		$1.34^{+0.12}_{-0.06}$	

¹⁰ ✓ means that the parameter can be determined by GRAVITY or RM data. Numbers in brackets after $\sqrt{}$ are median values with uncertainties of 90% confidence range from fittings of GRAVITY data for a convenient comparison. Values determined by the joint analysis are medians of the posterior distributions with uncertainties of 68% confidence ranges. RM¹⁰: one-dimensional reverberation mapping, in which only flux variations of broad emission lines are fitted. $\xi_{\text{BLR}} = R_{\text{BLR}}/D_*$ (the angular sizes) and $\zeta = (GM_*/R_{\text{BLR}})^{1/2} c^{-1}$ are reduced quantities for the fitting.



GRAVITY+ White paper



SDSS J092034.17+065718.0 $z=2.32$

GRAVITY+ collaboration, Nature (submitted), 2023

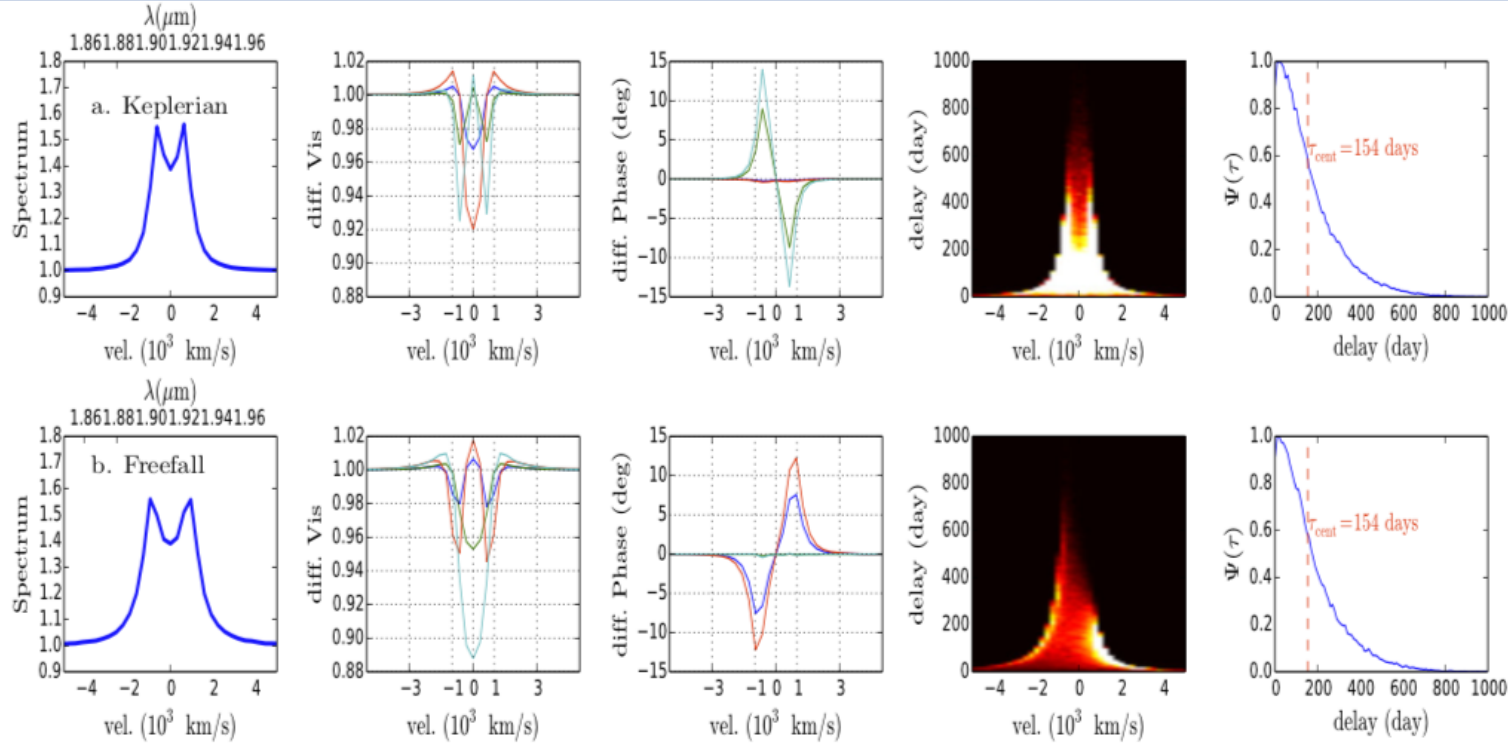


FIGURE 4.10: Spectrum (left), differential visibility (left-middle), differential phase (middle), 2D response function (middle-right), 1D response function (right) is plotted for different velocity profile for flat geometry case; Keplerian (upper row) and free fall inflow (lower row). OI observables are computed using baselines U1 (red), U2 (cyan), U3 (blue) and U4 (green).

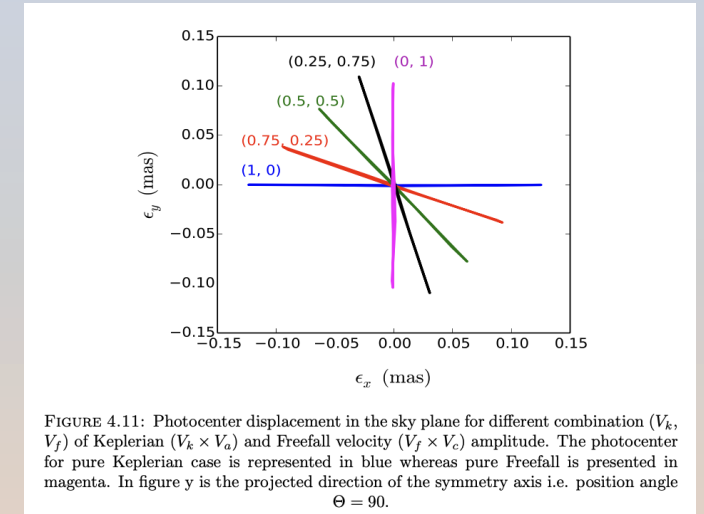
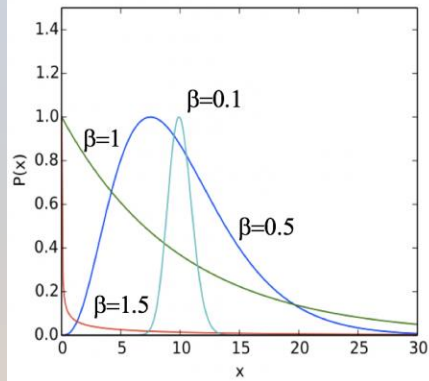


FIGURE 4.11: Photocenter displacement in the sky plane for different combination (V_k , V_f) of Keplerian ($V_k \times V_a$) and Freefall velocity ($V_f \times V_c$) amplitude. The photocenter for pure Keplerian case is represented in blue whereas pure Freefall is presented in magenta. In figure y is the projected direction of the symmetry axis i.e. position angle $\Theta = 90$.

Rakshit, Thesis, 2015

- Equivalent angular SA measures and equivalent linear RM measures are affected differently by parameters that introduce degeneracies on the mass and distance estimates:
 - Shape parameter, inner radius, **inclination**, opening angle,
 - **position angle**, kinematics (Keplerian, radial, turbulent...)
 - Clouds opacity...

SARM simulation with fixed line width, time lag, and differential phase amplitude (Rakshit, Petrov et al, 2015)



Chapter 4. Geometrical and kinematical model of BLR

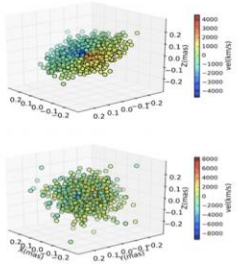
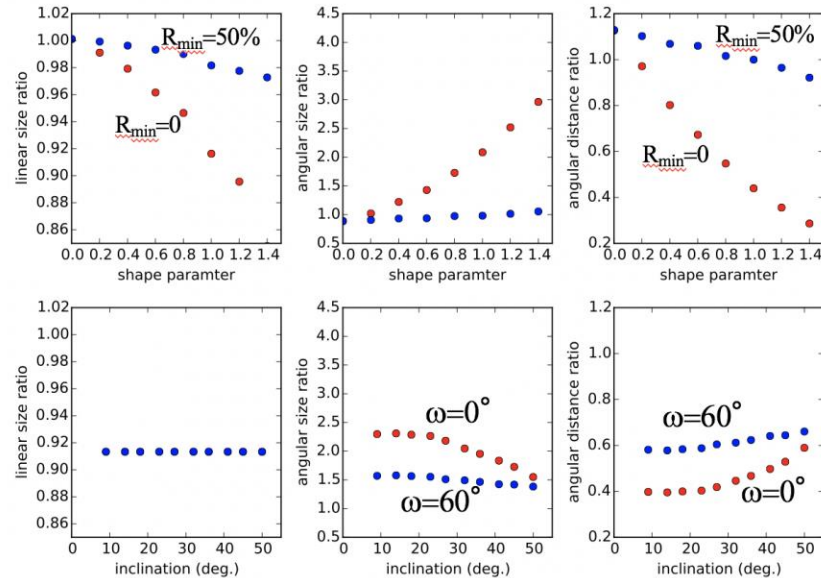


FIGURE 4.3: Cloud distribution with the velocity (km/s) in color code. $M_{\text{BH}} = 10^8 M_{\odot}$, $i = 30^\circ$, $R_{\text{in}} = 1000 R_g$, $\sigma_{\text{th}} = 0.1$ mas with flat Keplerian disk geometry $\omega = 0^\circ$ (upper plot) and spherical geometry $\omega = 90^\circ$ (lower plot).



Rakshit, thesis, 2015

Differential interferometry of QSO BLRs 7

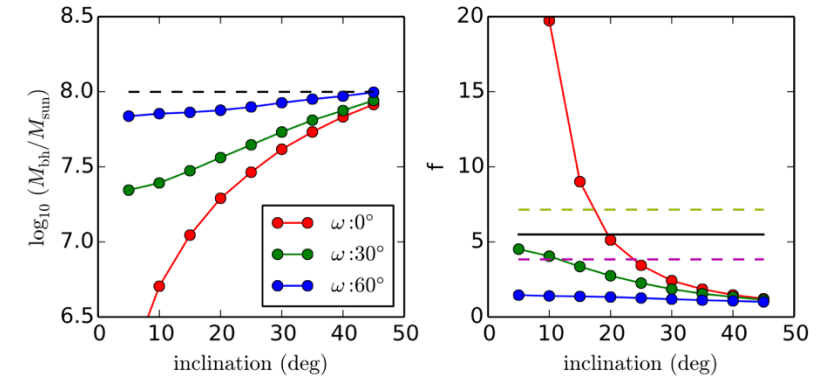
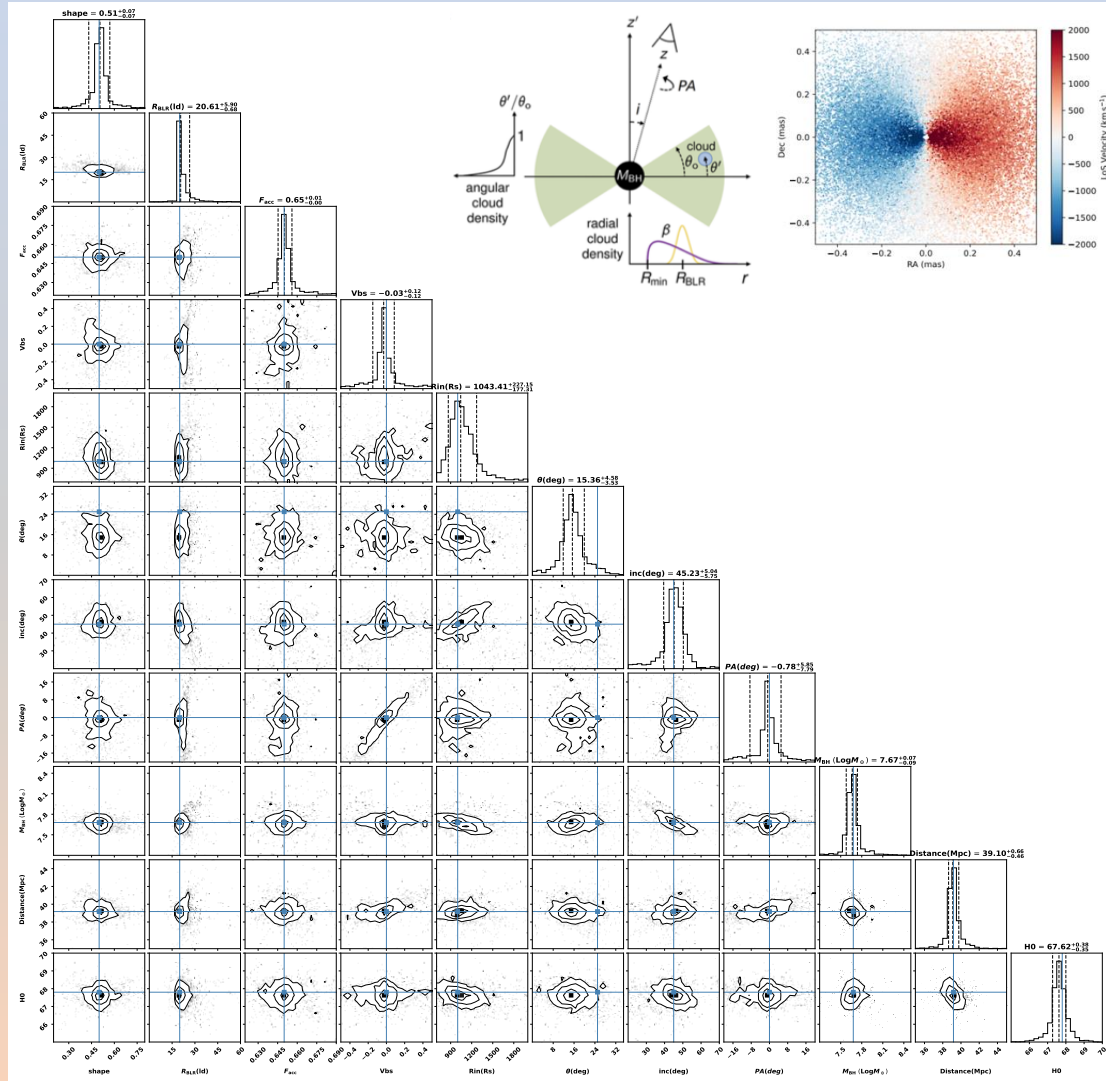


Figure 5. M_{bh} (left panel) and scale factor (right panel) as a function of inclination for different opening angles $\omega = 0^\circ$ (red), 30° (green) and 60° (blue). The input mass of this simulation is $10^8 M_{\text{sun}}$. We see that an error on i or ω can result in a very large mass error.

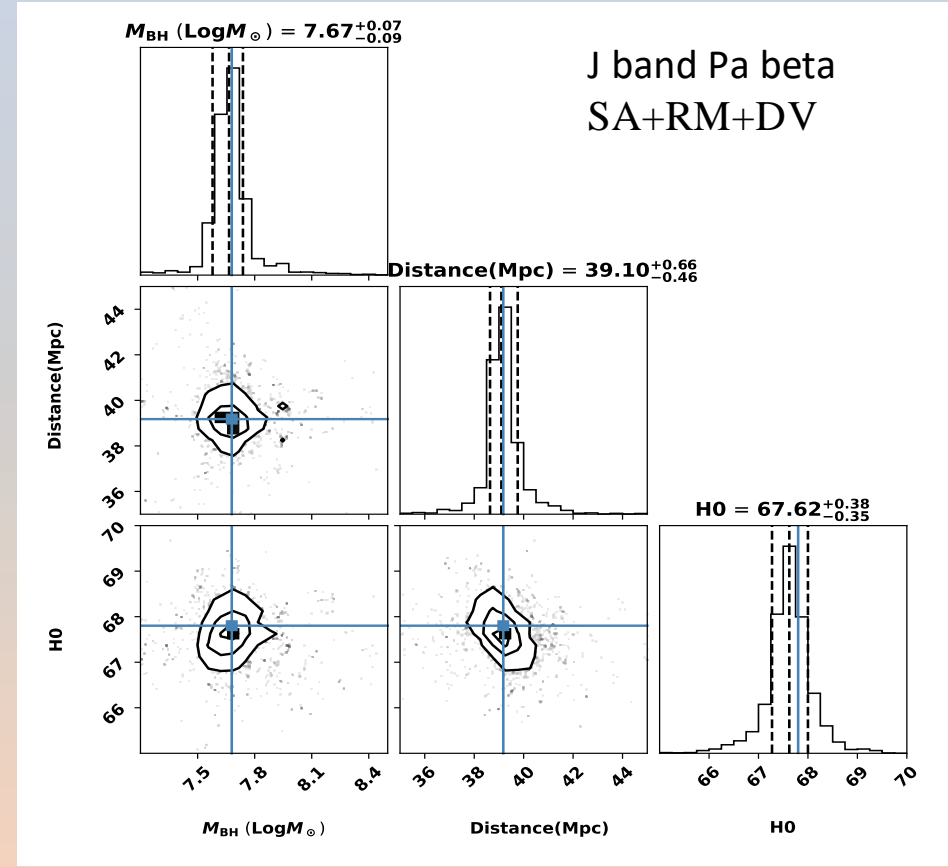
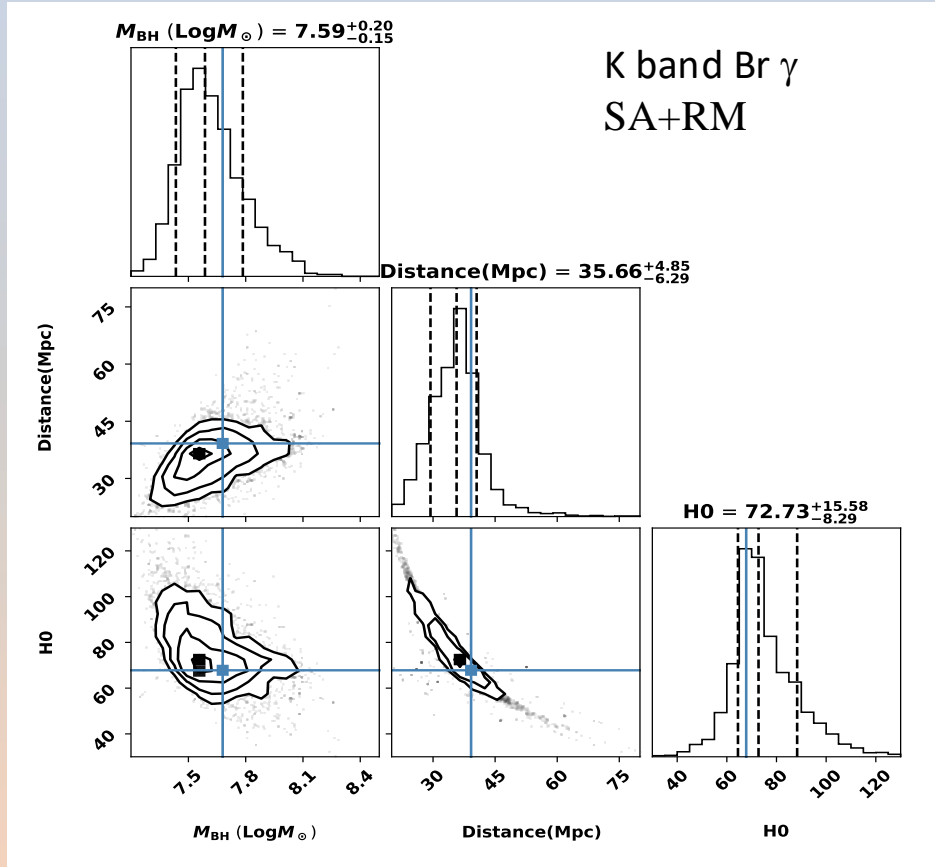
Rakshit+, MNRAS, 2015

BLR model and model fitting



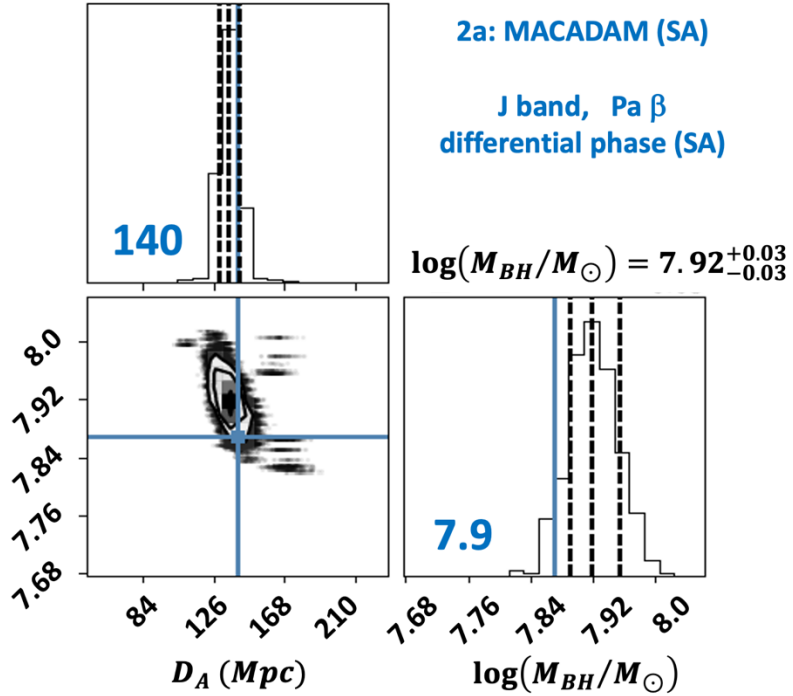
- Large “cloud list” axisymmetric model
 - Each cloud has a position, a velocity and emits a Doppler shifted emission line
 - Shape parameter of the radial distribution
 - Mean radius R_{BLR} in light days
 - Line/continuum ratio
 - Velocity ratio (tangential / radial)
 - Min radius R_{in}
 - Opening angle
 - Inclination
 - Position angle
 - Black hole mass M_{BH}
 - Distance
 - H0
-
- Turbulent velocity
 - Cloud opacity
 - Radial velocity power law parameter
 - ...

NGC 3783 39 Mpc $H_0=67.8$

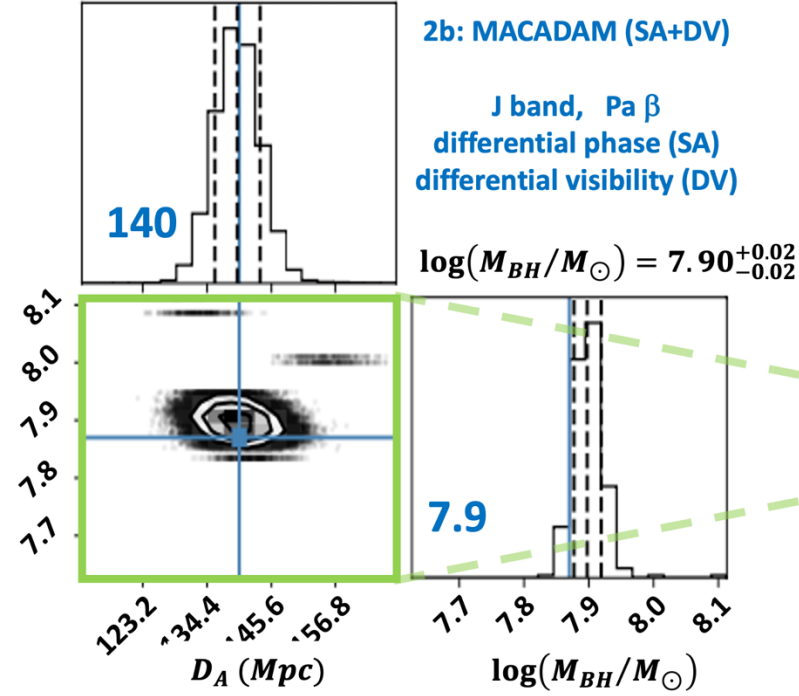


SA+RM and SA+RM+DV model fitting

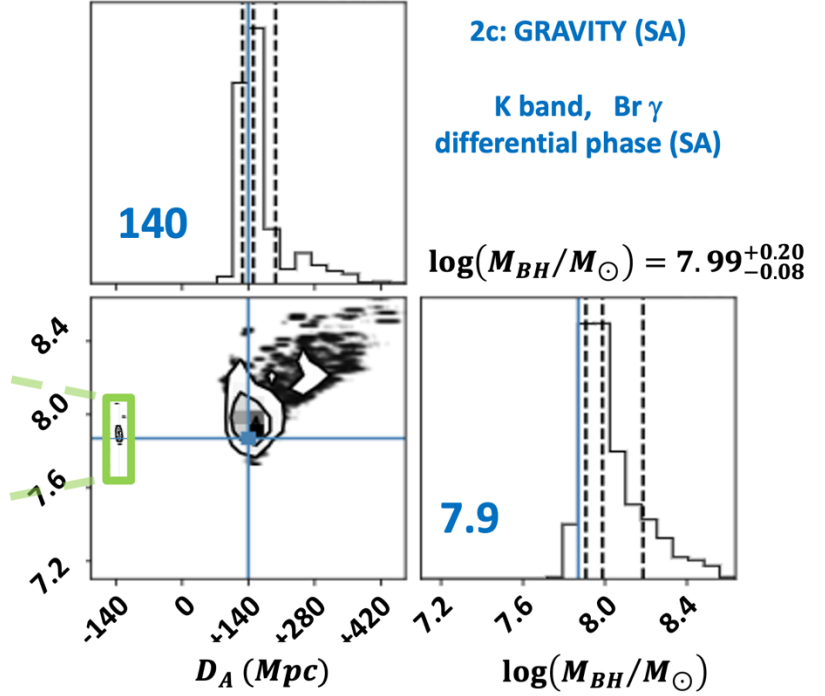
$$D_A = 134.7^{+6.1 (+15.3)}_{-5.4 (-15.0)} \text{ Mpc}$$



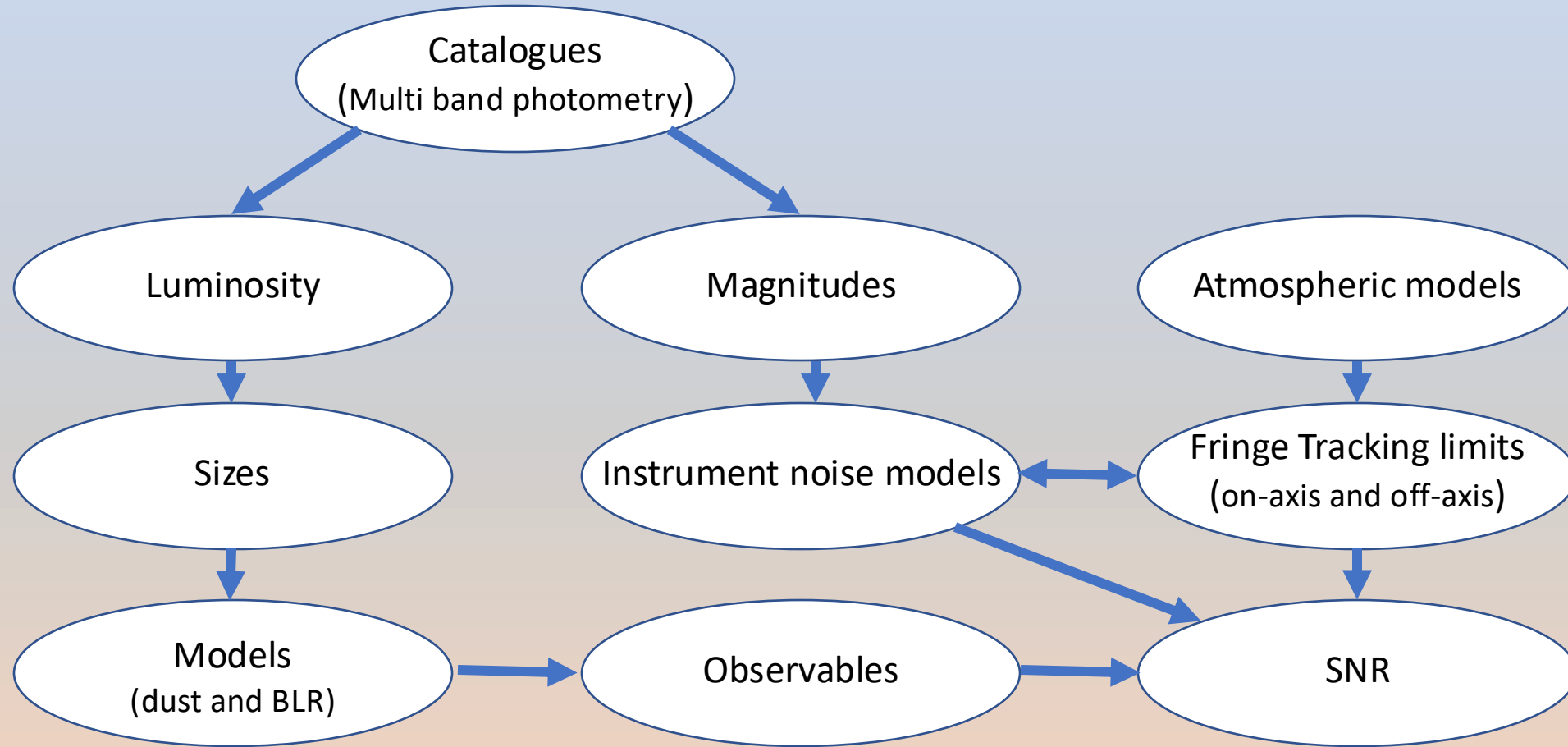
$$D_A = 139.6^{+3.97 (+14.5)}_{-3.87 (-14.5)} \text{ Mpc}$$



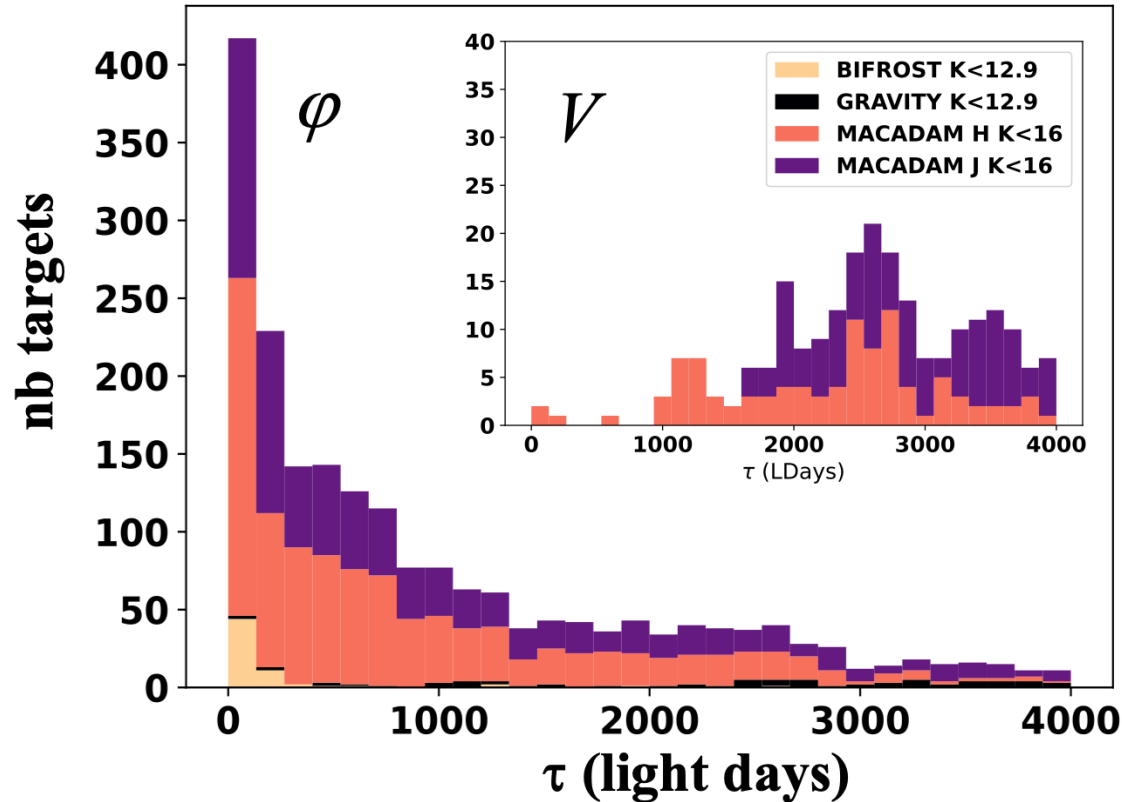
$$D_A = 150.4^{+47.6 (+49.6)}_{-22.7 (-26.7)} \text{ Mpc}$$



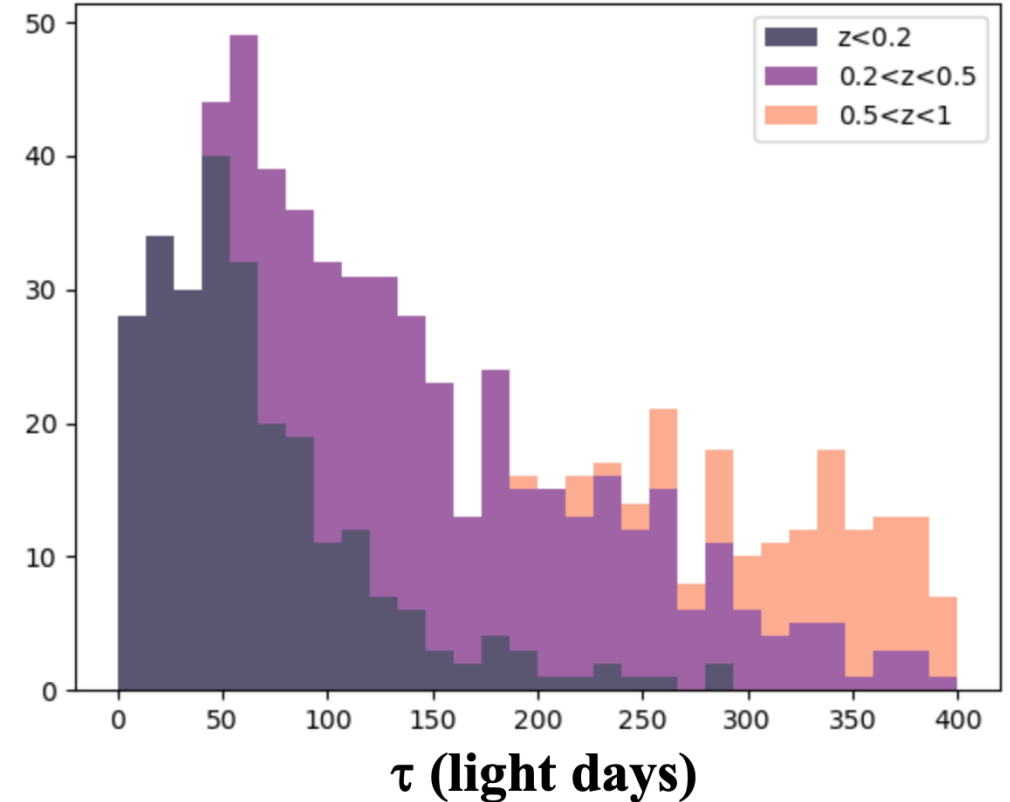
Selection of candidates



1a: Targets for SA (ϕ) and DV (V)



1b: MACADAM SA+RM targets



On-axis Fringe tracking. SNR>3 per spectral channel in 2 hours

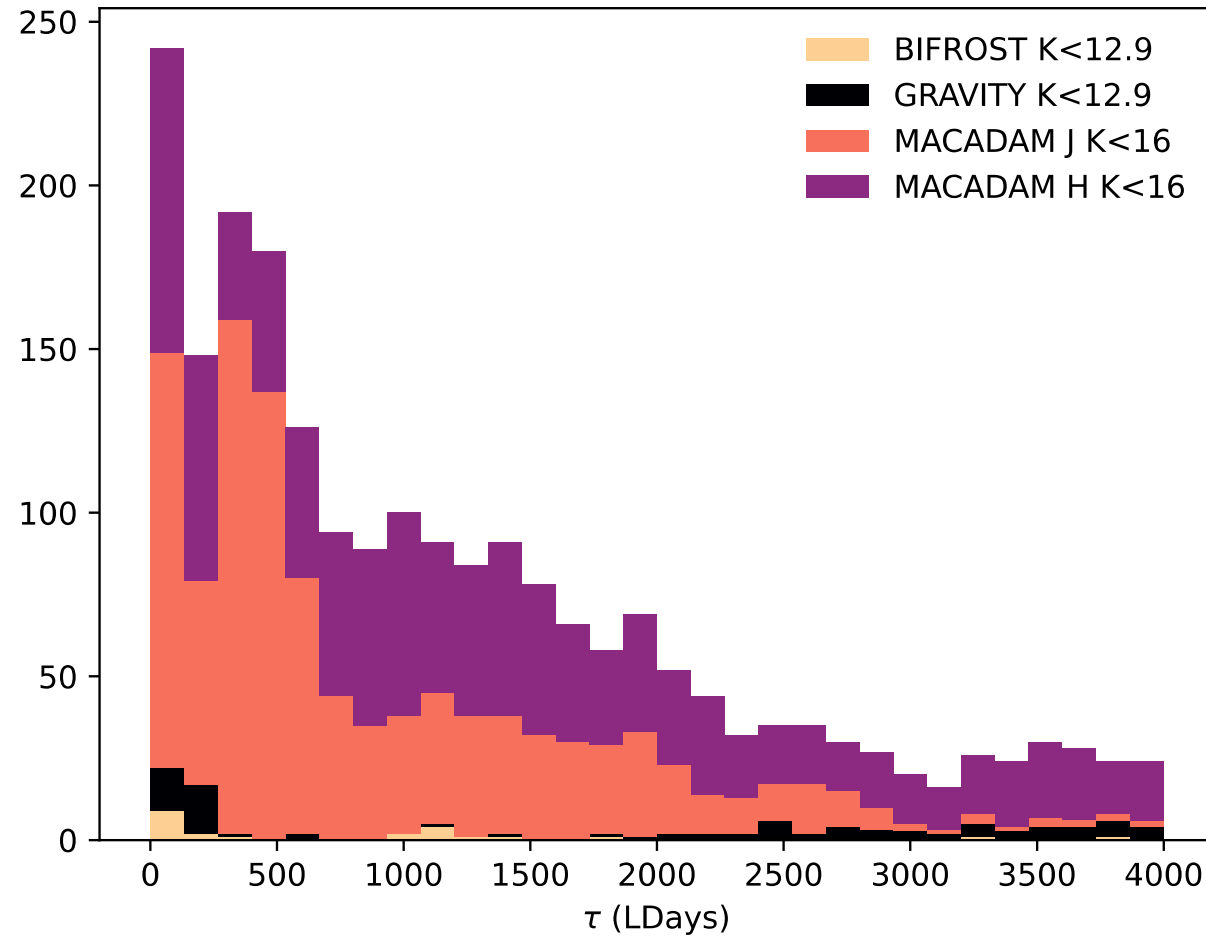
With off-axis fringe tracking

Off-axis tracking

188 K band targets
with $\tau < 4000$ days

30 K band targets with
 $\tau < 500$ days

SNR > 3 per spectral
channel in 4 hours

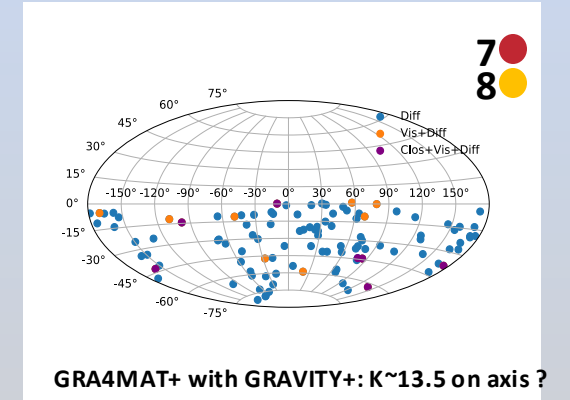
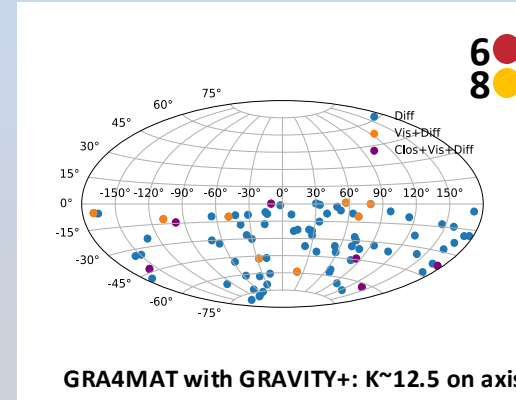
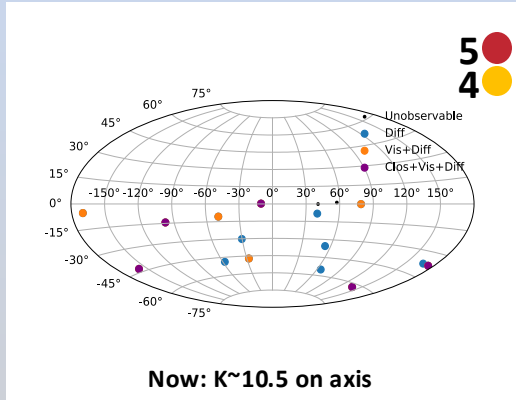


Measurables QSOs in L

Diff. Phase only

$$\pi \min \left(1, \frac{\Phi(\lambda_L)B}{\lambda_L} \right) SNR_C > 10$$

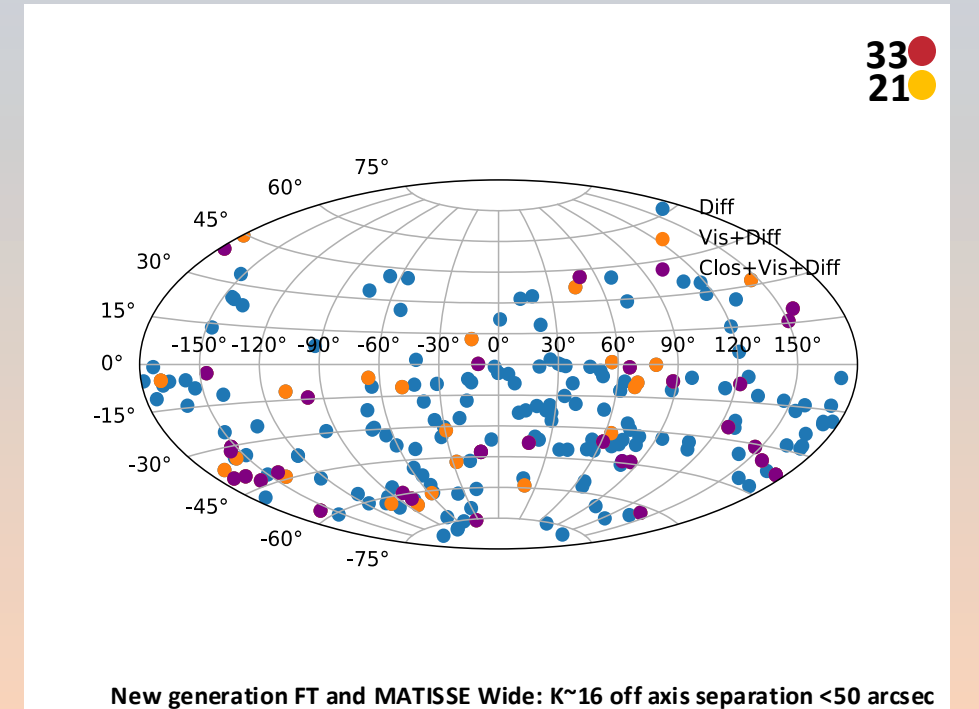
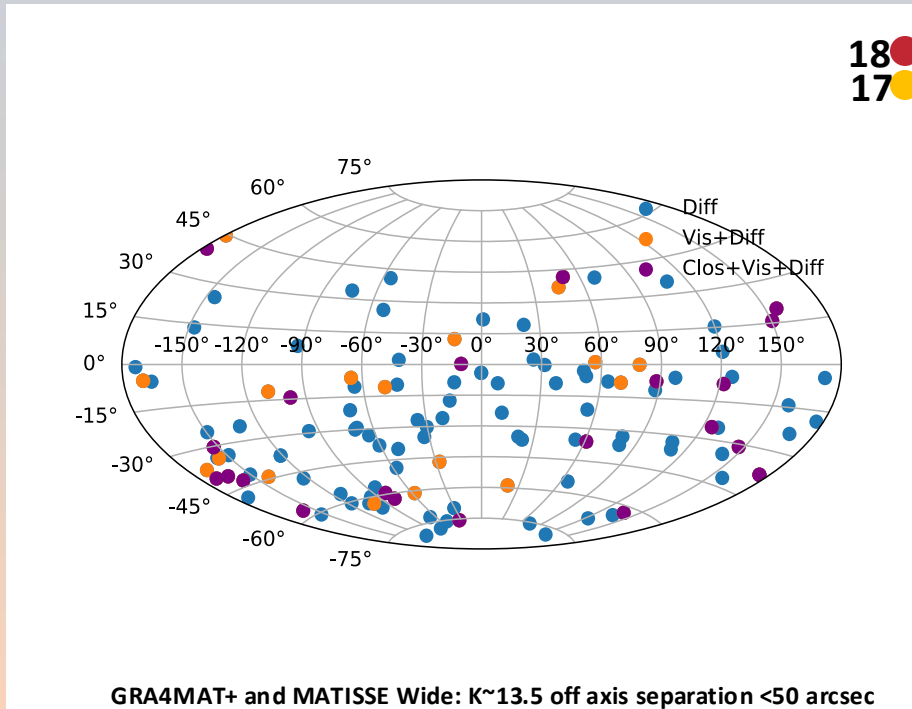
$$\Phi(\lambda_L) > 0.01 \frac{\lambda_L}{B} \text{ and } F_J > 4mJ$$



Vis. And Diff. Phase

$$\min \left\{ 1, \left[\frac{\Phi(\lambda_L)B}{\lambda_L} \right]^2 \right\} SNR_C > 10$$

$$\Phi(\lambda_L) > 0.08 \frac{\lambda_L}{B} \text{ and } F_J > 4mJ$$

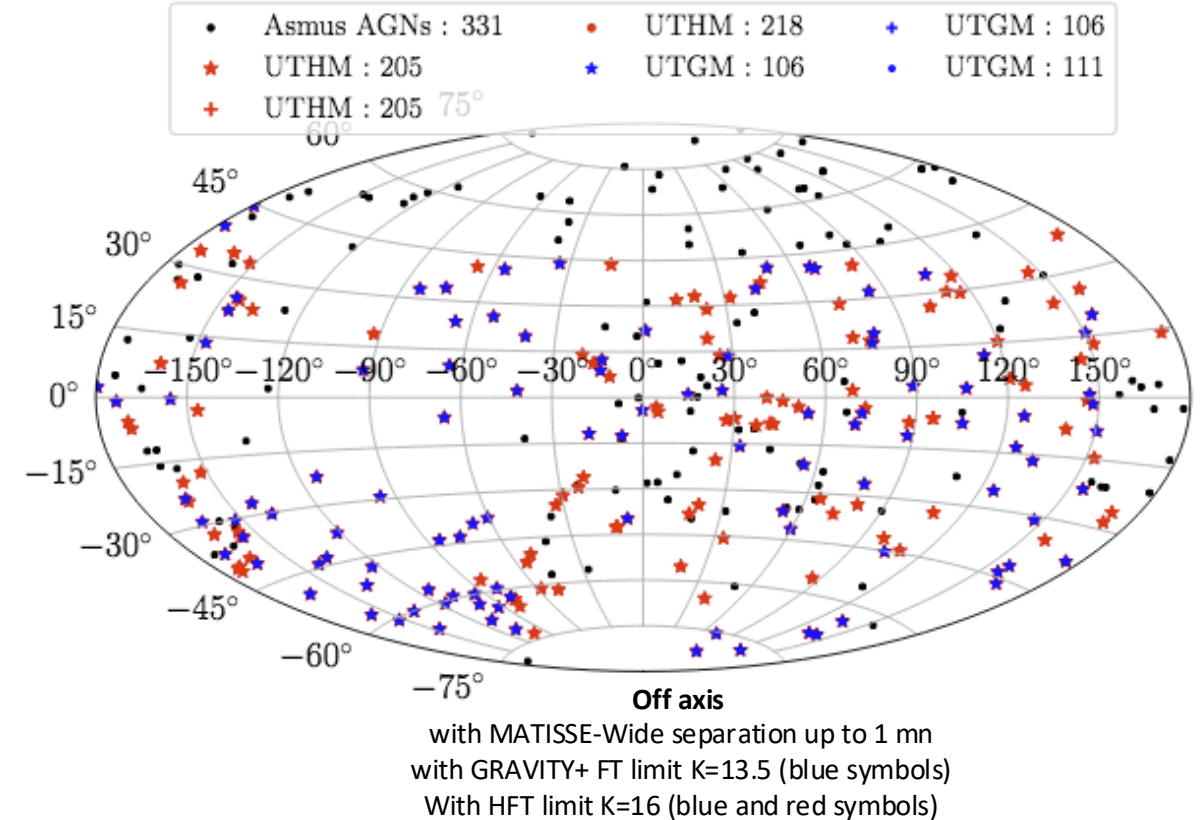
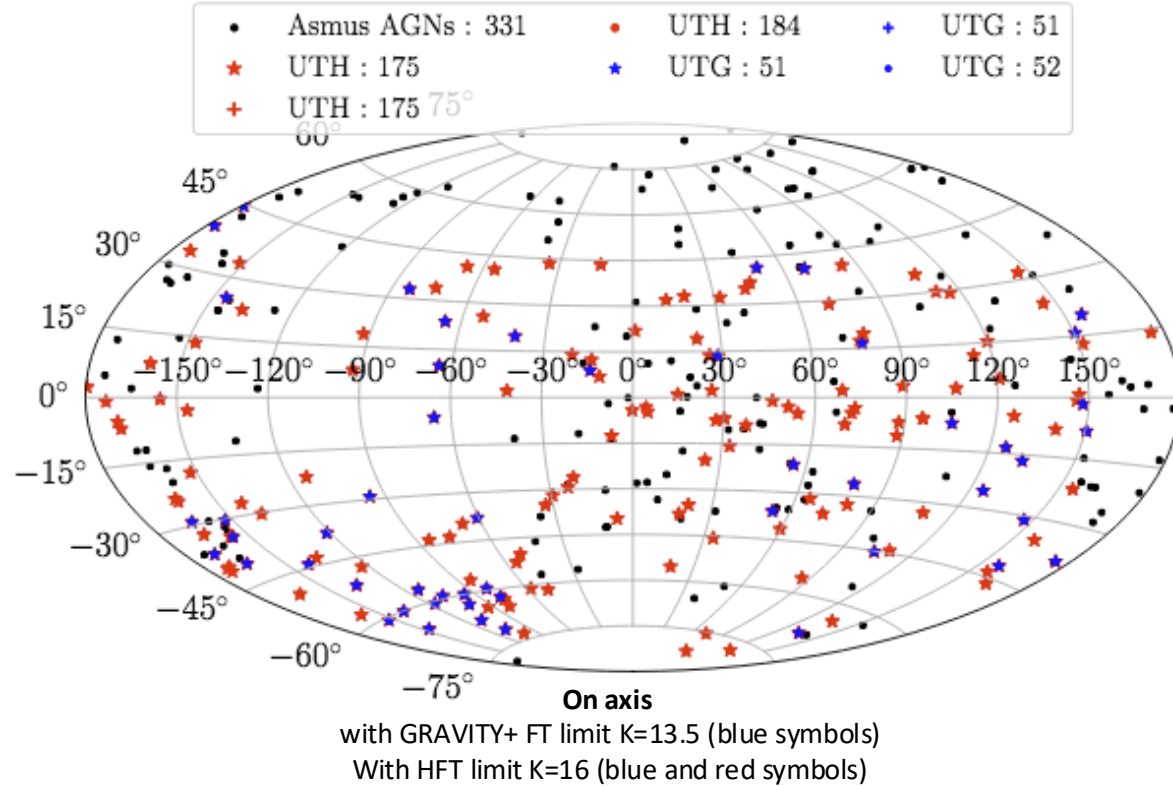


Closure Phase and all

$$\pi \min \left\{ 1, \left[\frac{\Phi(\lambda_L)B}{\lambda_L} \right]^3 \right\} SNR_C > 10$$

$$\Phi(\lambda_L) > 0.5 \frac{\lambda_L}{B} \text{ and } F_J > 4mJ$$

Nearby AGNs (<100 Mpc) observable in N



« * » : all measures, including closure phase, with good SNR

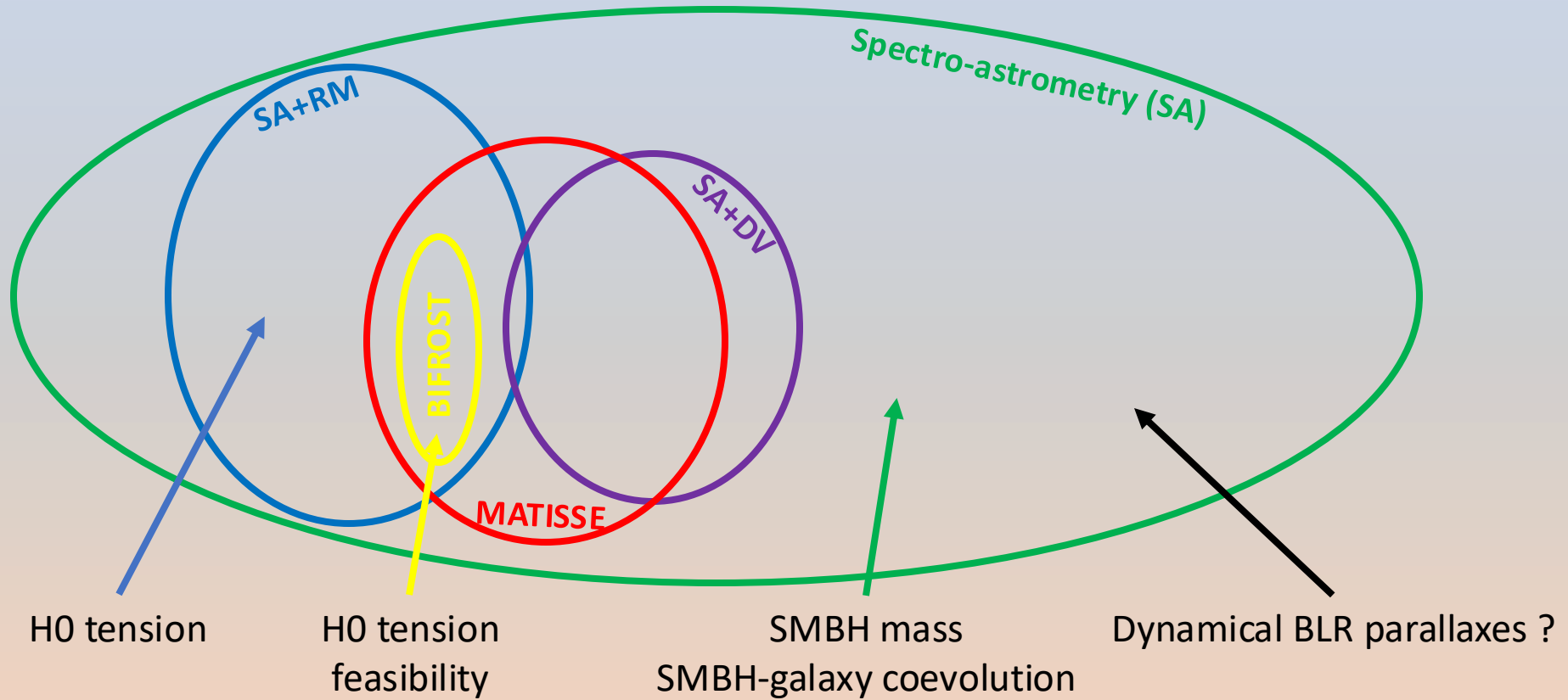
« + » : differential visibility and differential phase

« x » : differential phase only

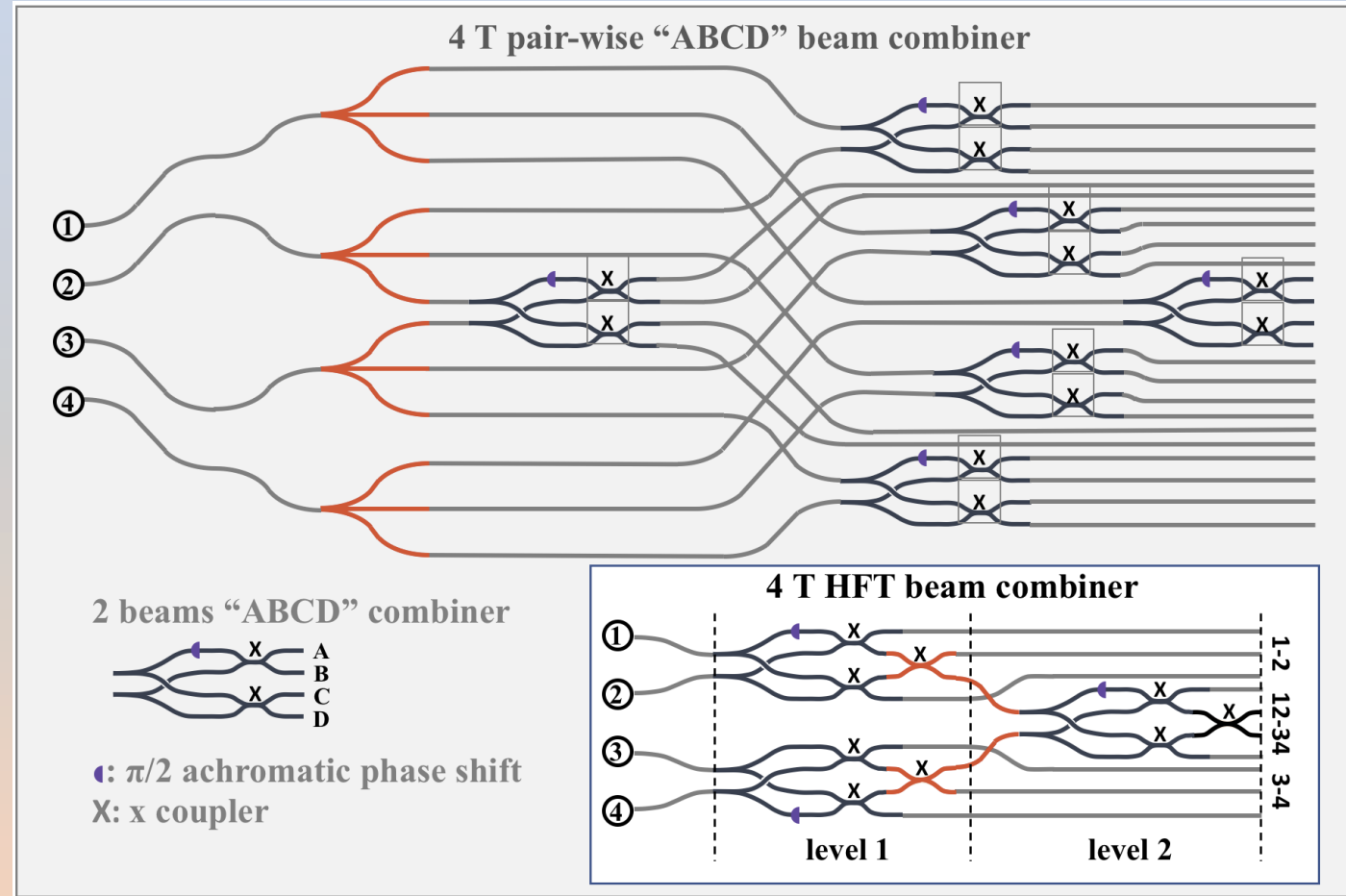
« . » : tracked but likely unresolved by science channel

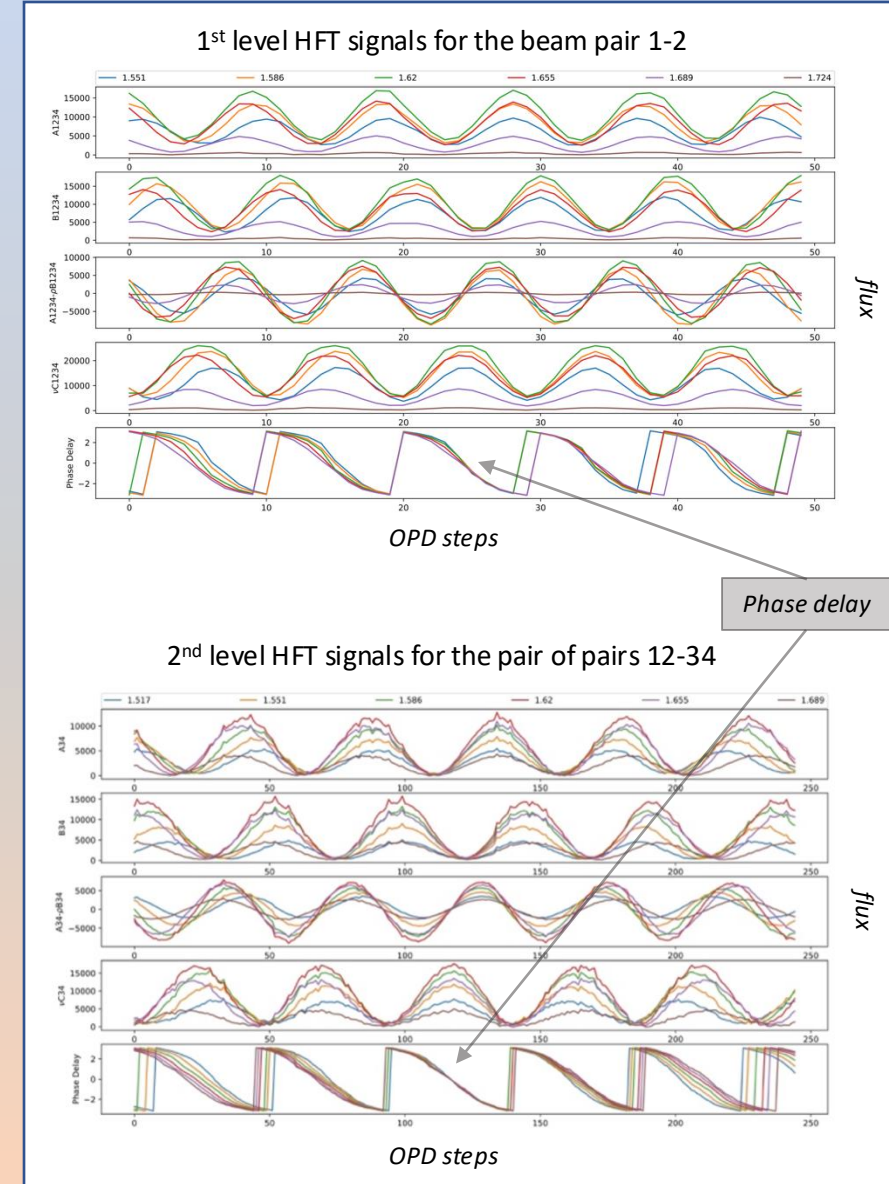
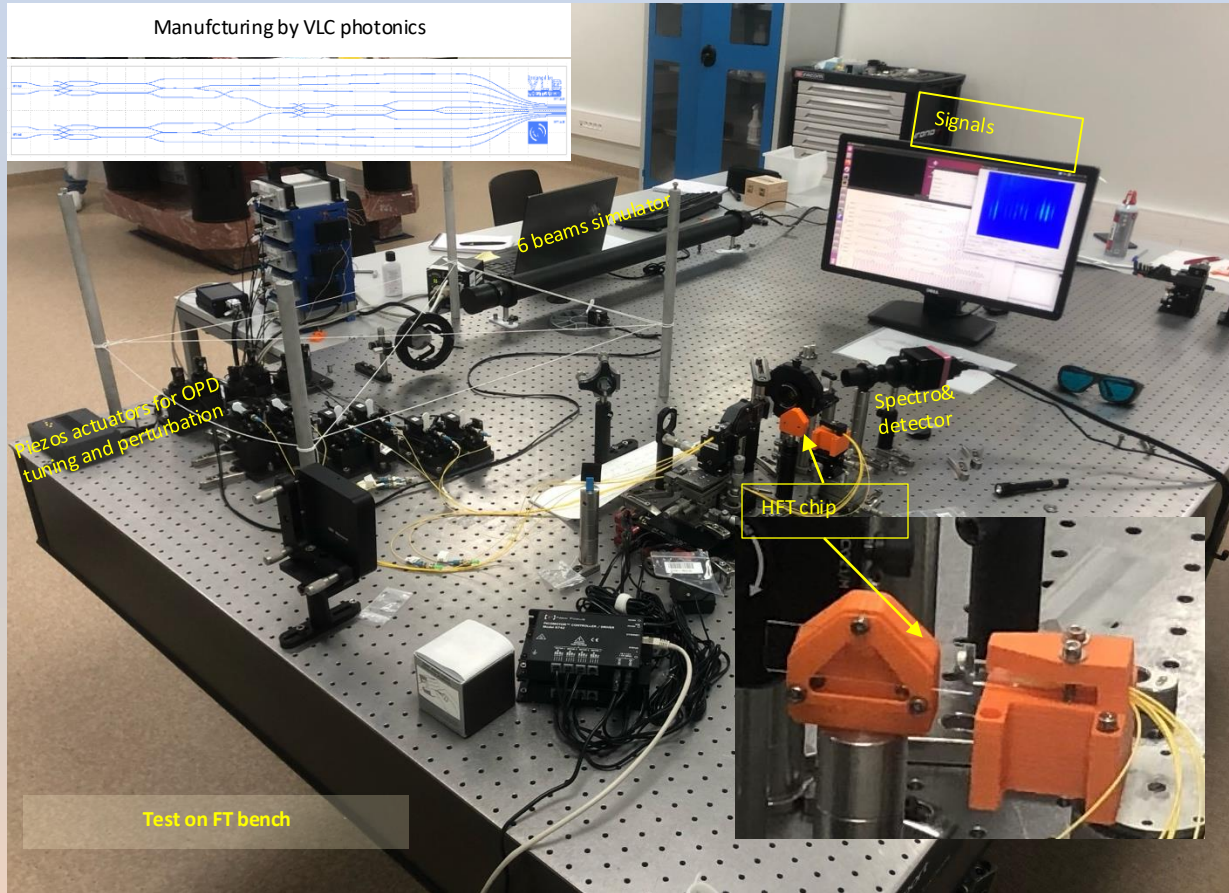
Based on estimated sublimation radius and N magnitude. See Boskri+, MNRAS, 2021 ([arXiv:2107.04729](https://arxiv.org/abs/2107.04729))

Method overlaps



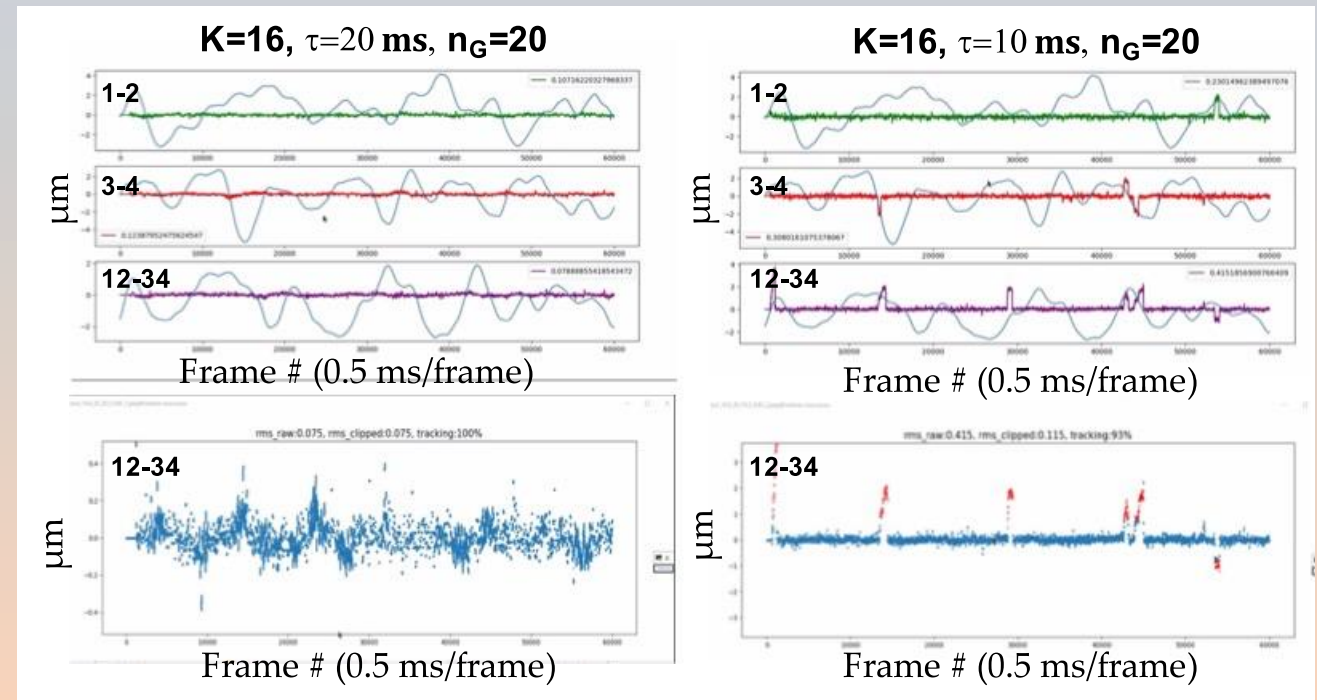
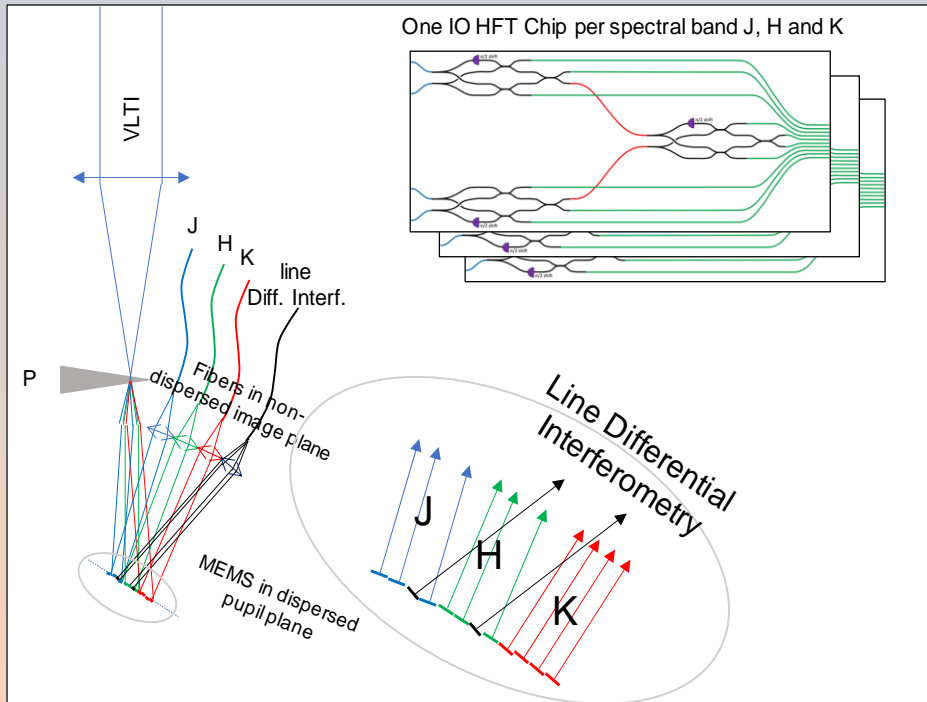
- Pair wise FT divide the flux of each telescope among $N_T - 1$ baselines and use $4(N_T - 1)$ measures to compute each piston
- HFT uses all flux of 2 Telescopes to cophase them with 3 measures (gain > 3 at 4T)
- Then uses the cophased fluxes to cophase pairs of pairs
- HFT chips use the same elementary building blocks than standard “ABCD” chips
- HFT chips are shorter and simpler → better transmission





Test on the bench and servo loop simulations validate the concept and confirm sensitivity gain

- HFT in J, H and K short (1.1 to 2.2 μm)
- One single mode chip per band
- On-axis: 90% of flux for FT. Off-axis: 100% flux for FT
- Optimized transmission but real VLTi J-H-K transmission and GPAO Strehl ratios
- K=15 sufficient for science goal



- Solving the H0 tension requires J and H bands and a gain in FT sensitivity limit ($K > 15$)
- BIFROST with FT limit=12.9 (visitor instrument) can be used to test the method and models.
- MATISSE could be used to constrain geometry of BIFROST targets
- Improved MATISSE models (with statistics over luminosity and Eddington ratio) are necessary and are being studied to study gas-dust interaction and constrain BLR geometry
- This requires MATISSE-Wide
- FT at magnitude $K > 15$ is well within reach on the VLTI in the GPAO context with a new generation fringe tracker